Breath Status Tracking using Commodity WiFi

Dongheng Zhang, Yang Hu, and Yan Chen
School of Information and Communication Engineering, University of Electronic Science and Technology of China
No. 2006, Xiyuan Ave., West Hi-Tech. Zone, Chengdu, Sichuan, China, 611713
Email: eedhzhang@std.uestc.edu.cn, {yanghu and eecyan}@uestc.edu.cn

***Abstract*—In this paper, we propose a contact-free breath tracking system, BreathTrack, to track the status of breath using the off-the-shelf WiFi devices by exploiting the phase variation of the channel state information(CSI). BreathTrack utilizes a reference antenna connected from the transmitter to resolve the phase distortions introduced by the hardware imperfection. Moreover, BreathTrack utilizes the sparse recovery method to find the dominant path in the multipath indoor environment and derive the corresponding complex attenuation coefficient. Then, the phase variation of the complex attenuation coefficient is utilized to extract the detailed breath status and the breath rate. Extensive experiments are conducted to show that BreathTrack could estimate the breath rate with the median accuracy of over 99% in most scenarios, and could track the detailed status of breath directly using the raw phase variation.**

I. Introduction

Breath rate is an important vital sign for health monitoring and medical diagnosis. While we have witnessed the increasing research interests and progresses in ubiquitous health monitoring in the past few years, most existing methods are intrusive that require the physical contact between human and sensors [1] [2] , which affects the normal breath of human and cannot be applied to the long-term breath monitoring.

To resolve this challenge, radio frequency based monitoring schemes that can provide non-intrusive breath rate estimation have been proposed. Vital-radio uses the frequency modulated continuous wave signal to estimate breath and heart rate[3]. However, such a system is not only expensive, but also occupies a large wireless band, which limits its application. To reduce the cost, the WiFi based breath estimation methods have been proposed[4], [5], [6], [8]. In [4], the UbiBreathe system has been proposed to utilize the Received Signal Strength (RSS) to monitor the breath signal. Since the RSS is not very sensitive to the minor displacements in the environment, it requires users to hold the WiFi devices close to their chests to achieve reasonable performance. The amplitude of channel state information (CSI) has also been utilized to estimate the breath rate [5] [6]. However, similar to the RSS, the amplitude is also not very sensitive to the minor displacement in the environment, due to which the estimation performance is limited. To achieve reasonable performance, sophisticated subcarrier selection, denoising and filtering progresses are needed. Since the frequency of breath varies in a very narrow band, i.e., about 0.2Hz, it is difficult to determine whether the estimated frequency is corresponding to the breath frequency.

Compared with the RSS and the amplitude of CSI, the phase of CSI is much more sensitive to the minor displacement in the environment, i.e., the phase of CSI is more suitable for breath rate estimation. However, the hardware imperfection of the commodity WiFi chips will introduce time-varying phase distortions, which makes it difficult to obtain accurate CSI phase information. It has been found that the phases of the measured CSIs across packets are not correlated even in very short time intervals [7]. Therefore, it is very difficult to estimate the breath rate directly from the phase variation of the measured CSI. To solve the phase distortion problem, the PhaseBeat system proposed in [8] utilizes the phase difference between antennas to eliminate the phase distortion. However, since the CSI measured on the antennas is affected by the minor displacement caused by breath, the phase difference between antennas is actually the subtraction of two periodic signals, which makes the model in [8] inaccurate.

Another challenge for the breath tracking in the indoor environment is the multipath effect. In a multipath indoor environment, the received signal is not periodic due to the aggregation of the multipath effect, and thus the breath rate cannot be directly obtained from the frequency components of the CSI. Moreover, the breath may be interrupted due to various factors such as talking, thinking or even some unconscious behaviors. In such a case, only the estimation of the breath rate may not be enough. Instead, it would be more significant if we could track the detailed breath status. However, to the best of our knowledge, there is no existing work that could reliably and accurately track the detailed breath status.

To resolve the challenges, in this paper, we propose a contact-free system using the off-the-shelf WiFi devices, BreathTrack, to track the human breath. BreathTrack exploits the phase variation of the CSI to track human breath. To avoid the phase distortions and obtain the accurate phase information, BreathTrack combines the hardware and software corrections. Specifically, the time-invariant PLL phase offset (PPO) is calibrated by the hardware correction using cables and splitters, while the time-varying carrier frequency offset (CFO), sampling frequency offset (SFO) and packet detection delay (PDD) are removed by the software corrections using the phase difference between the CSI at the receiver antennas and that at the reference antenna connected from the transmitter. To eliminate the multipath effect in the indoor environment, BreathTrack utilizes the sparse recovery method to find the

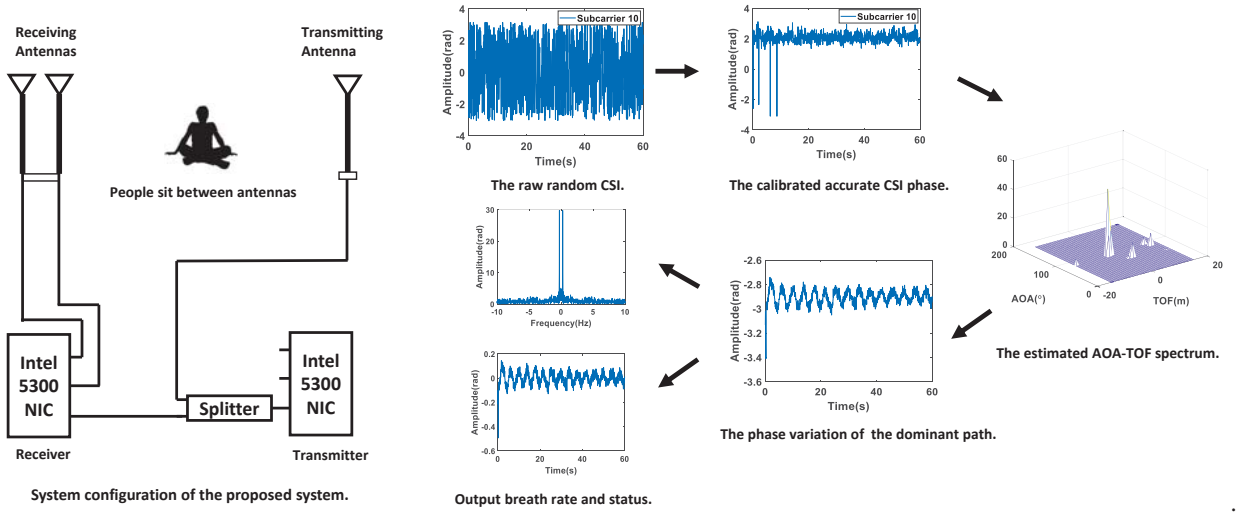

Fig. 1. An illustration of the BreathTrack system. The raw CSI is calibrated according to the signal of the reference antenna which is connected from the transmitter. Then, the AOA-TOF of received signal is jointly estimated with the sparse recovery method. After that, the phase variation of the dominant path is extracted. Finally, the breath rate and the breath status are output.

dominant path in the environment and obtain the corresponding complex attenuation coefficient of this dominant path from the CSI. Then, the phase variation of the complex attenuation coefficient is utilized to extract the detailed breath status and the breath rate. Extensive experiments are conducted to show that BreathTrack could estimate the breath rate with the median accuracy of over 99% in most scenarios. Besides the breath rate, BreathTrack is the first system which could track the detailed status of breath directly from the raw extracted phase using commodity WiFi chips.

The rest of the paper is organized as follows. Section II presents the theoretical model and the sparse recovery theory of the joint AOA-TOF estimation. In Section III, we illustrate in detail how to obtain accurate CSI phase and track the status of breath. The experimental results are shown in Section IV. Finally, conclusions are drawn in Section V.

II. Theoretical Model

In this section, we first present the CSI model of breath estimation and the challenges. Then, we introduce the CSI model of array signal processing. Finally, we illustrate how to extract the CSI phase variation caused by breath. The system model of BreathTrack is shown in Fig. 1.

A. CSI Model of Breath Detection

Let us first consider the ideal case without the multipath effect. In such a case, with the minor displacement caused by breath, the CSI affected by a static human can be rewritten as

$$y(t) = h_0 e^{-j2\pi \frac{d_0 + d(t)}{\lambda}}, \tag{1}$$

where d_0 is the time-invariant path length and $d(t)$ denotes the additional dynamic path length caused by breath. h_0 denotes the complex attenuation of the path, λ denotes the wavelength of the signal.

From (1), we can see that in the ideal case with a single path, the breath status can be derived directly from the phase variation of $y(t)$. However, in practice, there exists several propagation paths in typical indoor environment due to the multipath effect. In addition, the CSI would be perturbed by the noise introduced at the receiver, which is usually assumed to be additive white Gaussian noise. Thus, the CSI in the multipath environment can be expressed as

$$y(t) = \sum_{l=1}^{L} h_l e^{-j2\pi \frac{d_{l0} + d_l(t)}{\lambda}} + e(t), \tag{2}$$

where L denotes the number of propagation paths and $e(t)$ denotes the noise. When the l^{th} path is static, $d_l(t) = 0$.

According to (2), the CSI characterizes the multipath propagation environment. In such a case, without separating the signal affected by the human breath from the multipath summation, one may only estimate part of the frequency components of the breath signal rather than the whole time domain shape. Moreover, the phase of the measured CSI from the commodity WiFi chip is generally distorted due to the imperfect internal circuit, which further reduces the estimation accuracy. To resolve the above challenges, we propose to use the array signal processing techniques to address the multipath effect and adopt both the hardware and software correction methods to obtain accurate CSI from the commodity WiFi chip, which will be introduced in detail later.

B. CSI Model of Array Signal Processing

To resolve the challenge of multipath effect, we introduce array signal processing techniques to jointly estimate the angle of arrival(AOA) and the time of flight (TOF), then extract signal from the specific path based on the its AOA-TOF. We adapt sparse recovery based method which was shown to achieve better resolution [12], especially in the low SNR

scenarios [13] compared with previous works[11], [10]. In the following, we will show the formulation of AOA-TOF estimation .

Let θ_l and τ_l denote the AOA and TOF of the l^{th} path, respectively. Suppose that there are M antennas equipped in a uniform linear array with antennas space interval d, and K subcarriers with frequency interval Δf. Let α_l denote the complex attenuation of the signal from l^{th} path, which is assumed to be the same for all antennas and subcarriers. Thus, the relative phase between adjacent antennas and subcarriers of the l^{th} path can be expressed as

$$\Phi(\theta_l) = e^{\frac{-2\pi d \cos\theta_l}{\lambda}}, \tag{3}$$

and

$$\Phi(\tau_l) = e^{-j2\pi\Delta f\tau_l}. \tag{4}$$

Therefore, the joint phase shift from the CSI of the m^{th} antenna and the k^{th} subcarrier to that of the first antenna and the first subcarrier is given by

$$\Phi_{mk}(\theta_l,\tau_l) = exp\Bigg(-j2\pi\Big((k-1)\Delta f\tau_l + f_0\frac{(m-1)dcos\theta_l}{c} + (k-1)\Delta f\frac{(m-1)dcos\theta_l}{c}\Big)\Bigg), \tag{5}$$

where f_0 denotes the carrier frequency of the signal.

With M antennas and K subcarriers, the phase shift vector can be written as

$$a(\theta_l,\tau_l) = [1\ \Phi_{21}(\theta_l,\tau_l)\ ...\ \Phi_{mk}(\theta_l,\tau_l)\ ...\ \Phi_{MK}(\theta_l,\tau_l)]^T. \tag{6}$$

Combing all the L paths, the steering matrix is defined as

$$A = [a(\theta_1,\tau_1), a(\theta_2,\tau_2), ..., a(\theta_L,\tau_L)]. \tag{7}$$

Thus, considering the measurement error caused by noise, the measured CSI can be expressed as

$$y = \sum_{l=1}^{L} a(\theta_l,\tau_l)\alpha_l + e = A\alpha + e, \tag{8}$$

where α_l denotes the complex attenuation of the signal from the l^{th} path.

To cast (8) into a sparse recovery problem, let us define a AOA-TOF grid as follows

$$\overline{\theta\tau} = [\overline{(\theta_1,\tau_1)}, \overline{(\theta_2,\tau_2)}, ..., \overline{(\theta_N,\tau_N)}], \tag{9}$$

where N denotes the number of grid points. The overline is introduced to distinguish the grid points and actual paths.

Similar to (6), the phase shift vector of the grid can be written as

$$\overline{a(\theta_n,\tau_n)} = [1\ \Phi_{21}(\theta_n,\tau_n)\ ...\ \Phi_{mk}(\theta_n,\tau_n)\ ...\ \Phi_{MK}(\theta_n,\tau_n)]^T. \tag{10}$$

According to (7) and (10), the new steering matrix which contains all the grid points can be written as

$$\overline{A} = [\overline{a(\theta_1,\tau_1)}, \overline{a(\theta_2,\tau_2)}, ..., \overline{a(\theta_N,\tau_N)}], \tag{11}$$

Thus, the received signal and the complex attenuation vector can be expressed as

$$y = \overline{A}\overline{\alpha} + e, \tag{12}$$

with $\overline{\alpha}$ being the complex attenuation vector

$$\overline{\alpha} = [\alpha_1, \alpha_2, ..., \alpha_N], \tag{13}$$

where α_n equals to the complex attenuation coefficient if there exists signal with the AOA of θ_n and TOF of τ_n, otherwise, α_n equals to zero. Thus, there are at most L non-zero elements which correspond to the L paths. Apparently, the number of grid points can be much larger than L, i.e., $L \ll N$, which means that $\overline{\alpha}$ is a sparse vector. As a result, the problem can be solved using minimum norm methods [12], and the optimization problem can be formulated as follows

$$\begin{aligned} &\min \quad ||\overline{\alpha}||_1, \\ &s.t. \quad ||y - \overline{A}\overline{\alpha}||_2^2 \le \beta, \end{aligned} \tag{14}$$

where β is the parameter determined by the noise level. Once the minimal norm problem was solved, we can obtain A from $\overline{A}$ by selecting the columns of which α_n is non-zero.

C. Breath rate estimation based on sparse estimation

In this section, we will introduce the way to enhance the robustness of AOA-TOF estimation and derive the phase variation caused by breath. Since the AOA-TOF changes slowly compared with the speed of transmitting packets, we are motivated to combine the samples at different slots to obtain robust estimation. However, combining the samples at different slots directly would increase the computation cost dramatically, which makes it unapplicable to practical systems. To resolve the problem, we utilize the l_1-SVD algorithm proposed in [12] to improve the accuracy and robustness of the AOA-TOF estimation. The l_1-SVD algorithm [12] is a tractable approach to use a large number of time samples coherently. The idea is to decompose the data matrix into the signal and noise subspaces, and reformulate the problem with reduced dimensions into the multiple sample sparse spectrum estimation problem.

Let Y denote T consecutive time samples of $y(t)$. Taking the SVD on Y, we have

$$\mathrm{Y} = \mathrm{U}\Sigma\mathrm{V}'. \tag{15}$$

Let us keep the reduced $MK \times L$ dimensional matrix $\mathrm{Y_{SV}} = \mathrm{U}\Sigma\mathrm{D_L} = \mathrm{YVD_L}$, where $D_L = [I_L 0']$, I_L is a $L \times L$ identity matrix, and 0 is a $L \times (T-L)$ matrix of zeros. Similarly, let X and E denote T consecutive samples of $\alpha(t)$ and $e(t)$, respectively, and define $\mathrm{X_{SV}} = \mathrm{XVD_L}$ and $\mathrm{E_{SV}} = \mathrm{EVD_L}$. Then, we have

$$\mathrm{Y_{SV}} = \mathrm{AX_{SV}} + \mathrm{E_{SV}}. \tag{16}$$

With the SVD, the size of the problem is reduced from T blocks of data to L, where $L \ll T$. Note that the form of (16) is the same as that of (8), which means that it could be effectively solved by the minimal norm method [12]. Although the formulation of SVD uses the information about

the number of paths, L, it has been observed that incorrect determination of L has no catastrophic consequences [12]. Once we obtain the estimation of AOA-TOF, the complex attenuation coefficient can be derived, which is given by

$$\alpha(t) = A^{\dagger} y(t), \tag{17}$$

where $A^{\dagger}$ denotes the pseudo-inverse of A. Note that A is the steering matrix in (7), which is obtained in the last subsection by jointly estimating AOA-TOF and selecting the columns of $\overline{A}$ where the corresponding complex attenuation coefficient is non-zero. The phase variation of $\alpha(t)$ corresponds to the minor displacement caused by breath directly, which can be utilized to track the breath.

III. Data Processing

In this section, we will introduce in detail the data processing steps of the proposed system. Specifically, we first introduce how to obtain accurate CSI. Then, we present how to extract the phase corresponding to the breath and how to estimate the breath rate.

A. Obtaining accurate CSI for breath detection

Due to the hardware imperfection of commodity WiFi chips, the measured CSI is generally distorted by the internal circuit. Moreover, some distortions even change rapidly with time, which makes it difficult to obtain the accurate CSI measurement. Existing work has found that the phases of measured CSIs across packets are not correlated [7], which limits the application of phase variation based wireless sensing. According to [17], there are mainly four kinds of phase distortions: Carrier Frequency Offset (CFO), Sampling Frequency Offset (SFO), Packet Detection Delay (PDD) and PLL Phase Offset (PPO).

With the four kinds of phase distortion mentioned above, the actual measured CSI can be expressed as

$$\begin{aligned} y_{m,k}(t) &= e^{-j2\pi(f_{CFO}t + k\Delta f(\tau_{SFO}(t)+\tau_{PDD}(t))} \\ &\quad e^{j\varphi_{PLL_m}} \sum_{i=1}^{L} \alpha_i e^{-j2\pi f_k \tau_i^m}, \end{aligned} \tag{18}$$

where τ_{PDD} and τ_{SFO} denote the time shift introduced by PDD and SFO, respectively, f_{CFO} denotes the CFO, and φ_{PLL} denotes the time-invariant PPO.

The correction of the PPO has been well investigated in [9] and [10]. Since the calibration is only invoked when the receiver sets the channel, to guarantee the robustness of the phase correction, we use the method proposed in [9] which utilizes cables and splitters to correct the PPO between antennas.

While the PPO is a constant offset which can be corrected through cables and splitters, other phase distortions (CFO, SFO and PDD) are difficult to correct since they are time-variant. To the best of our knowledge, there is no existing reliable correction approach up to now. The most recent approach in [18] utilized two propagation paths to get rid of the phase distortion. However, such a method is not reliable since it is very difficult to detect two paths stably in the indoor multipath environment using the off-the-shelf WiFi devices. Fortunately, we have found that the CFO, SFO and PDD are the same among different antennas, which makes the phase difference between antennas time-invariant in the static environment [8]. To create an artificially static environment, we connect the transmitter and receiver by a coaxial cable. By assuming that the antenna 1 at the receiver is connected with the transmitter, the measured CSI on the antenna 1 at the receiver can be expressed as

$$\begin{aligned} y_{1,k}(t) &= e^{-j2\pi(f_{CFO}t + k\Delta f(\tau_{SFO}(t)+\tau_{PDD}(t))} \\ &\quad e^{j\varphi_{PLL_1}} \alpha_0 e^{-j2\pi f_k \tau_0}, \end{aligned} \tag{19}$$

where α_0 and τ_0 denote the complex attenuation of the coaxial cable and the TOF in the cable, respectively.

Since the signal propagates in the coaxial cable, on the ideal case, the CSI measured on this antenna should be time-invariant. Thus, the variation of the measured CSI is only caused by the distortions, i.e., the CFO, SFO and PDD. With such information on this antenna, to eliminate the phase distortion on other antennas, the measured CSI of m^{th} antenna is multiplied with the complex conjugate of the CSI on the antenna 1 as follows

$$\begin{aligned} \hat{y}_{m,k} &= (y_{1,k})^* \times y_{m,k} \\ &= \alpha_0 e^{j2\pi f_k \tau_0} \sum_{i=1}^{L} \alpha_i e^{-j2\pi f_k \tau_i^m}, \end{aligned} \tag{20}$$

where $*$ denotes the operation of complex conjugate. Note that since φ_{PLL} can be removed as illustrated above, we omit it in (20).

We can see that the modified CSI $\hat{y}_{m,k}$ is the ideal CSI $y_{m,k}$ multiplied with a constant complex coefficient. Since τ_0 is known which is determined by the length of coaxial cable, the complex coefficient will not affect the estimation of AOA-TOF and thus not affect the estimation of the breath.

B. Phase Extraction and Breath Rate Estimation

With the modified CSI $\hat{y}_{m,k}$ in (20), we utilize the sparse recovery algorithm in Section III to estimate the AOA-TOF of the paths in the environment. According to [14], it can be derived that the the proposed algorithm could not perfectly obtain the accurate AOA-TOF estimation of all paths due to the limited number of antennas and bandwidth. Luckily, it can be derived theoretically and verified experimentally that the estimation for the dominant path is accurate. Thus, we only pick the path with the maximum amplitude in the estimated AOA-TOF spectrum to build matrix A in (7). Then, the complex coefficient of this dominant path is obtained, and the phase of this complex coefficient is extracted for breath rate estimation.

Benefiting from the aforementioned phase extraction algorithms, the breath rate estimation does not require sophisticated denoising, filtering and/or approximating processing steps as in the previous works[4], [5], [6], [8]. Since the DC component of the phase variation is large, which may affect the breath rate

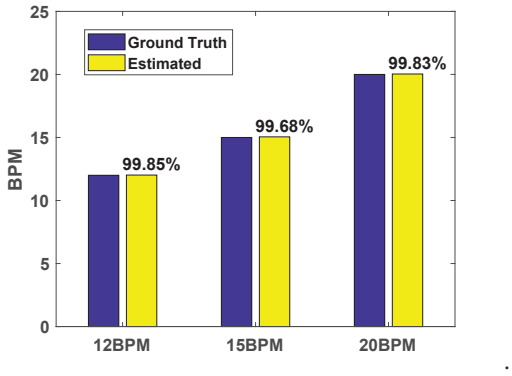

Fig. 2. Median error of breath rate estimation under different breath frequencies.

estimation, we utilize the Hampel Filter to remove it [8]. The window size is set as 100 samples and the threshold is set to be 0.01. To further suppress the low frequency noise, we use a FIR highpass filter with the cutoff frequency 0.05Hz, which is determined by the lowest breath frequency of human. Then, we simply pick the peak of FFT spectrum of the filtered phase data as the estimation of breath rate.

IV. Experiments Results

In this section, we conduct extensive real experiments to evaluate the performance of the proposed system.We use two desktop computers equipped with the Intel 5300 NIC as the transmitter and the receiver. The Linux 802.11n CSI Tool [16] is installed on both the transmitter and the receiver. We randomly choose channel 62, i.e., 5.31GHz center frequency with the 40MHz bandwidth, as our experimental band. The receiver is equipped with a uniform linear array which is composed of three omnidirectional antennas, while we only use two of them since one of the port is connected with the transmitter directly. The space interval of the antennas is 2.6cm, which is about the half wavelength. The transmitter sends 20 packets per second using one omnidirectional antenna. The transmitted signal is first divided into two parts using a microwave power splitter: one is fed into the transmit antenna and the other is fed into an attenuator which is connected with the receiver via a coaxial cable. The AOA-TOF estimation problem with the sparse recovery formulation is solved using the CVX tool [15]. The AOA grid spans $[1°, 180°]$ with $N_\theta = 90$ and the TOF grid spans $[-15m, 15m]$ with $N_\tau = 31$.

A total of 8 different participants were invited. The performance of the system is evaluated by comparing the estimated breath rate with the ground truth. To obtain the ground truths, participants are asked to synchronize their breaths with the metronome on their cellphones. Besides the controlled breath, participants are also asked to breath naturally and count their breaths manually. Experiments are conducted in a $5m \times 8m$ meeting room.

The transmitter and the receiver are separated 2m away. The participant sits in the midpoint of the transmitter and the receiver. To show the robustness of the proposed system, they are asked to breath with the frequency of 0.2Hz, 0.25Hz and 0.33Hz in different experiments, respectively. The median accuracy of the breath rate estimation of three frequencies is shown in Fig. 2. We can see that the proposed method can achieve very accurate breath rate estimation, above 99.5%, in this scenario.

Since most existing methods seem to have reasonable performance in estimating the breath rate under simple settings, to show the advantages of the propose system, we compare the raw phase variation data of different subcarriers and the raw phase extracted by the proposed system. We first ask the participant to breath with 15 BPM and the results are shown in Fig. 3. It can be seen clearly from the Fig. 3 (a) that there are 15 periods. On the contrary, although the phase of the subcarriers do show some periodicity, it is difficult to recognize the breath period based on the phase variation on the subcarriers as shown in Fig. 3 (b), (c), and (d). Note that we do check the phase variation of all different subcarriers, however, none of them could be used to judge the breath period. In all experiments of the proposed system, the raw phase data is directly related to the breath and the frequency of the breath can be easily estimated in the way similar to Fig. 3 (a). In contrast, sophisticated subcarrier selection, denoising and filtering progresses are needed in previous works[4], [5], [6], [8]. Since the frequency of breath varies in a very narrow band, i.e., about 0.2Hz, it is difficult to determine whether the estimated frequency is corresponding to the breath frequency.

To further illustrate the advantages of proposed system, we show two more experiments in Fig. 4 and Fig. 5. Since the status of human breath may change rapidly due to many factors, such as speaking, moving or even some unconscious behaviors, it will be much more significant if one could identify the whole breath status rather than just estimate the rate. In Fig. 4, the participant is asked to hold the breath for 30s first, then take a deep breath, and finally breath normally. In Fig. 5, the participant is asked to breath normally first, and then hold the breath. As shown in Fig. 4 (a) and Fig. 5 (a), the proposed system can perfectly capture such minor and fast change of the whole breath status. However, similar to the results in Fig. 3, we cannot judge the breath status directly from the phase variation on different subcarriers as shown in (b), (c), and (d) of Fig. 4 and Fig. 5.

V. Conclusion

In this paper, we proposed BreathTrack, the first system that can track the detailed status of breath using the off-the-shelf WiFi devices. To achieve this, we proposed hardware and software correction methods to remove both the time-invariant and time-varying phase distortions introduced by the hardware imperfection of commodity WiFi chips and thus obtain the accurate CSI. We also proposed a joint AOA-TOF sparse recovery method to eliminate the multipath effect in the indoor environment and extract the information of the dominant path to track the status of breath. Experimental results show that

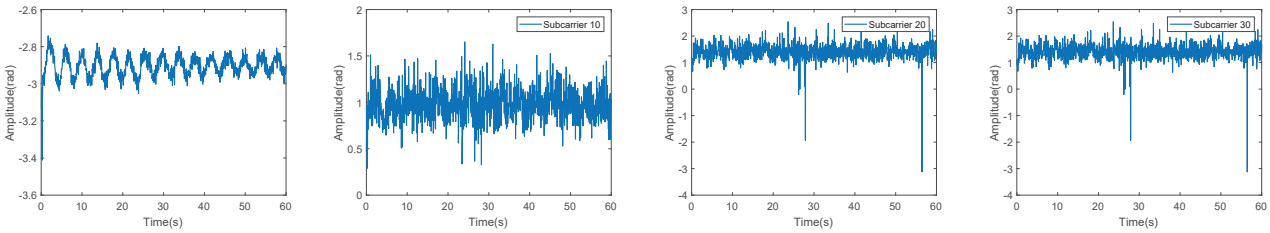

(a) Raw phase extracted by the proposed method. (b) Raw phase of the CSI on subcarrier 10. (c) Raw phase of the CSI on subcarrier 20. (d) Raw phase of the CSI on subcarrier 30.

Fig. 3. The case when one person breaths 15 times per minute.

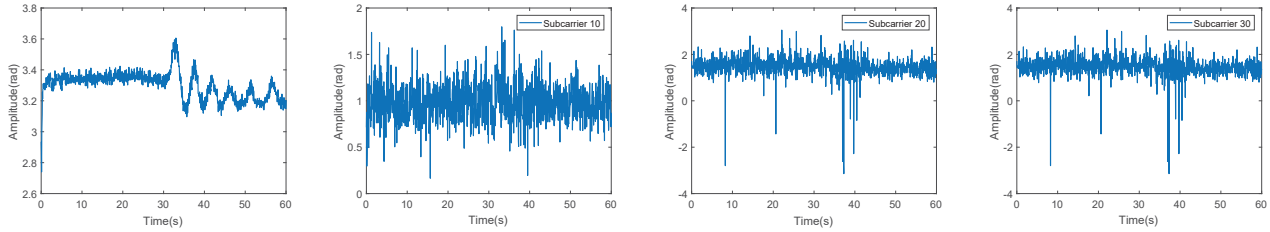

(a) Raw phase extracted by the proposed method. (b) Raw phase of the CSI on subcarrier 10. (c) Raw phase of the CSI on subcarrier 20. (d) Raw phase of the CSI on subcarrier 30.

Fig. 4. The case when one person holds the breath first and then breath normally.

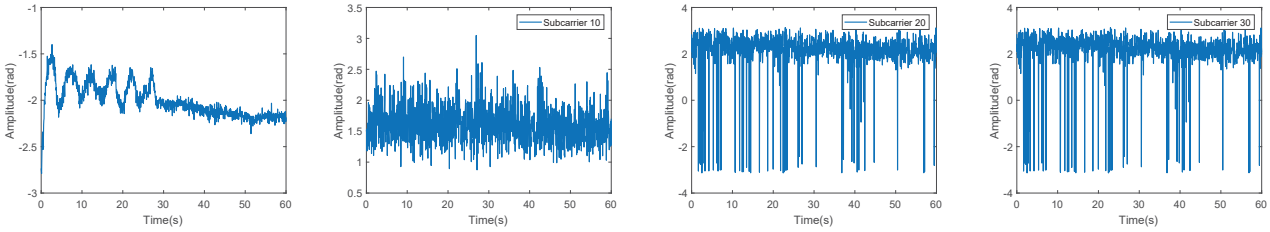

(a) Raw phase extracted by the proposed method. (b) Raw phase of the CSI on subcarrier 10. (c) Raw phase of the CSI on subcarrier 20. (d) Raw phase of the CSI on subcarrier 30.

Fig. 5. The case when one person breaths normally first and then holds the breath.

BreathTrack can achieve high accurate breath rate estimation and track the detailed status of breath.

REFERENCES

[1] iBabyGuard. **http://www.ibabyguard.com/**.

[2] VivoSense. **https://www.vivosense.com/portfolio/equivital/**

[3] F. Adib., H. Mao, Z. Kabelac., D. Katabi and R. C. Miller. "Smart homes that monitor breathing and heart rate," *ACM CHI*, 2015.

[4] H. Abdelnasser, K. A. Harras and M. Youssef, "UbiBreathe: A Ubiquitous non-Invasive WiFi-based Breathing Estimator", *ACM MobiHoc* 2015.

[5] J. Liu, Y. Wang, Y. Chen, J. Yang, X. Chen, and J. Cheng. Tracking Vital Signs During Sleep Leveraging Off-the-shelf WiFi. *ACM MobiHoc* 2015.

[6] X. Liu, J. Cao, S. Tang, J. Wen, and P. Guo, "Contactless Respiration Monitoring Via Off-the-Shelf WiFi Devices", *IEEE Trans. Mobile Comput.*, vol. 15, no. 10, pp. 2466-2479, 2016.

[7] R. Nandakumar, B. Kellogg, and S. Gollakota. "Wi-fi gesture recognition on existing devices." arXiv:1411.5394, 2014.

[8] X. Wang, C. Yang and S. Mao, "PhaseBeat: Exploiting CSI phase data for vital sign monitoring with commodity WiFi devices," *IEEE ICDCS*, 2017.

[9] J. Xiong and K. Jamieson, "ArrayTrack: A Fine-Grained Indoor Location System," *USENIX NSDI*, 2013.

[10] J. Gjengset, J. Xiong, G. McPhillips, and K. Jamieson. "Phaser: enabling phased array signal processing on commodity WiFi access points," *ACM MobiCom*, 2014.

[11] M. Kotaru, K. Joshi, D. Bharadia, and S. Katti, "Spotfi: Decimeter Level Localization Using WiFi," *ACM SIGCOMM*, 2015.

[12] D. Malioutov, M. Cetin, and A. S. Willsky, "A sparse signal reconstruction perspective for source localization with sensor arrays," *IEEE Trans. Signal Process.*, vol. 53, no.8, Aug. 2005

[13] W. Gong and J. Liu, "Robust indoor wireless localization using sparse recovery," *IEEE ICDCS*, 2017.

[14] Eldar Y C, Kuppinger P, Bolcskei H. "Block-sparse signals: Uncertainty relations and efficient recovery," *IEEE Trans. Signal Process.*, vol. 58, no. 6, pp. 3042-3054, June 2010

[15] CVX solvers, http://cvxr.com/cvx/doc/solver.html.

[16] D. Halperin, W. Hu, A. Sheth, and D. Wetherall, "Tool release: gathering 802.11n traces with channel state information," *ACM SIGCOMM CCR*, 2011.

[17] Y. Zhuo, H. Zhu, H. Xue, and S. Chang. "Perceiving Accurate CSI Phases with Commodity WiFi Devices," *IEEE INFOCOM*, 2017.

[18] M. Kotaru and S. Katti, "Position Tracking for Virtual Reality Using Commodity WiFi," *IEEE CVPR*, 2017.